# Solid-state effects on Coulomb capture and x-ray cascade of negative muons

H. Daniel, F. J. Hartmann, and R. A. Naumann*
*Physik-Department, Technische Universität München, D-85747 Garching, Germany*
(Received 22 June 1998)

Coulomb capture and the subsequent muonic x-ray cascade have been measured for a selection of solid-state targets: three allotropic forms of selenium, magnesium chloride with and without crystal water, and single-phase Nb-Ta alloys in three different stoichiometric ratios. Small but statistically significant differences were found in higher-level crossover transition x-ray intensities in Se. A rather large enhancement of crossover transition intensities was observed in magnesium chloride with water, which is ascribed to transfer from hydrogen. No significant variations with composition were found in the Lyman intensity patterns from Nb-Ta; the per-atom capture ratio was measured to be constant within 5%. [S1050-2947(99)08103-2]

PACS number(s): 36.10.Dr, 34.50.Bw

## I. INTRODUCTION

The availability of high-quality beams of negative muons at modern intermediate energy accelerators enables detailed tests of mechanisms involved in the terminal stopping and capture of heavy negative particles. It is now generally agreed that the capture event occurs when the kinetic energy is less than some tens of eV. Under these circumstances it is not surprising that the details of the valence electronic and lattice structures of the solid-state stopping target can decisively influence the capture mechanisms. However, the initial bound state in hydrogen-containing systems was shown to be predominantly of atomic and not of molecular nature [1].

There are numerous examples for the influence of the chemical environment on the intensity pattern of muonic x rays and on the probability for atomic capture into the components of chemical compounds: The $K_\beta$ to $K_\alpha$ intensity ratio from oxygen in the oxides of the third-row elements was found to change by more than 20% when going from magnesium oxide to phosphorous oxide, and to depend linearly on the ionicity [2,3]. The per-atom capture ratio in oxides was detected to be strongly influenced by the oxidation state of the bond partner in the oxide [4]. The angular-momentum distribution $P(\ell)$ of muons in muonic-atom states with large principal quantum number $n$, populated during the exotic particle cascade, was found to vary from a rather steep, nearly statistical distribution $[P(\ell) \propto 2\ell+1]$ for the simple compounds $Fe_2O_3$ or $FeCl_3$, to a nearly flat distribution for the more complex compound $K_3Fe(CN)_6$, be it in the solid state or in an aqueous solution [5].

In this laboratory, the bulk of our research has employed, in addition to elements, simpler ionic salts or metallic systems as stopping targets. Here the solid-state structure comprises individual ionic cores. Our data for these systems support the idea that in the solid state details of the capture process involving any particular atomic core are essentially constant [6].

Evidence of differing x-ray cascade intensities when negative muons are stopped in solid allotropic modifications of the same element or compound was first presented by Tauscher *et al.* from CERN for Se [7]. Another indication of such behavior came from the study of muon capture in the cubic and hexagonal forms of boron nitride (BN) by Knight *et al.* [8] at Los Alamos. The subsequent experiments by Schneuwly *et al.* at Paul Scherrer Institute established, in agreement with Ref. [8], differences both for capture and cascade for each BN allotrope [9].

Representing more or less similar work by others [7,8] we want to outline the findings of the Fribourg group in some detail. Clear differences were measured both for the relative intensities of the nitrogen muonic $K$ x-ray series, and for the per-atom muon capture ratio $A$(B,N). The former effect appeared as a progressive attenuation for the cubic form of the relative intensity through the higher members of the nitrogen Lyman series. This amounted to about 20% attenuation for the $6\rightarrow1$ nitrogen member. Additionally, the capture ratio $A$(B,N) measured for the cubic form was found to be about 18% lower relative to that for the hexagonal form. Simultaneously, the Fribourg group reported variations in relative intensities of muonic $K$ x rays emitted from various carbon targets: soot, graphite (hexagonal layered lattice) and diamond (tetrahedrally bonded cubic lattice). It is interesting to note that the carbon $K$ x-ray intensities from the cubic form were again observed to be progressively attenuated relative to the hexagonal form. This amounted to an approximate 15% effect at the $6\rightarrow1$ carbon Lyman member.

In another study, the Fribourg group [10] has reported relative intensity variations between the muonic $K$ x-ray series emitted from elemental phosphorus targets in the white (lattice with discrete tetrahedral $P_4$ subunits) and red or black forms (cross-linked extended chains of P atoms). The $K$ x rays from the more symmetrical white form were again found to be progressively more attenuated relative to those from either of the two chain forms. The attenuation reported for the $8\rightarrow1$ member corresponded to an intensity $0.885 \pm 0.069$ and $0.813 \pm 0.063$ relative to the intensity of the red and black forms. No attenuation effects were noted for the phosphorus muonic $L$ x-ray series.

In the same study [10], the Fribourg group measured muonic x-ray intensities from two allotropic forms of selenium. The intensities emitted from targets in the disordered

*On leave from Princeton University, Princeton, NJ. Present address: Dartmouth College, Hanover, NH.

 

red form ($Se_8$ molecular rings) and the black form (spirals formed of Se chains) were compared. A statistically significant attenuation effect was reported for both $7\rightarrow1$ (25% effect) and $8\rightarrow1$ (40% effect) transitions for the red form relative to the black. However, unlike the previous cases, the attenuation seemed to onset abruptly, at variance with older work at CERN [7]. For the Balmer series, no statistically significant intensity effects were observed, although there was some indication of a relative enhancement of the $10\rightarrow2$ and $11\rightarrow2$ members for the red form compared to the black. Accordingly, we wished to reexamine the muonic x-ray intensities from selenium targets for possible allotropic effects.

A completely different question is whether, and if so to what extent, the per-atom capture ratio $A(Z_1,Z_2)$ into atoms of atomic numbers $Z_1$ and $Z_2$ depends on the concentrations $k_1=k(Z_1)$ and $k_2=k(Z_2)$ for a single-phase alloy. Clearly the chemical forms of the atoms $Z_1$ and $Z_2$ are independent of the stoichiometric ratio $S=k_1/k_2$. Although often tacitly assumed, the independence of $A(Z_1,Z_2)$ of $S$ is not at all trivial: the shape of the spectral flux density spectrum $n(W)$ of the muons with energy $W$ within the targets may very well depend on $S$, and influence both the angular momentum distribution of the captured muons $P(I_0)$, with an effect on the cascade, and the capture ratio $A(Z_1,Z_2)$; this may be seen for $A(Z_1,Z_2)$ in the following way [11]. Underlaying the continuous-energy-loss model, the product of $n(W)$ and stopping power $\tilde{S}(W)\equiv -dW/d(\rho x)$, where $\rho$ is the target density and $x$ the path length, is a constant. Hence low stopping power means high spectral flux density, and vice versa. The per-atom capture ratio $A(Z_1,Z_2)$ is given by the ratio of the two capture integrals, namely, by

$$A(Z_1,Z_2)=\frac{\int_0^\infty \sigma_1(W)n_1(W)dW}{\int_0^\infty \sigma_2(W)n_2(W)dW}, \tag{1}$$

where $\sigma_i(W)$ and $n_i(W)$ are the capture cross section and the spectral flux density for atoms with $Z_i$, respectively, and $i=1$ and 2. $A(Z_1,Z_2)$ is related to the directly measured capture ratio $R(Z_1,Z_2)$ by

$$A(Z_1,Z_2)=\frac{1}{S}R(Z_1,Z_2). \tag{2}$$

$n_i(W)$ in Eq. (1) may here be expected to be the same, $n(W)$, both for $Z_1$ and $Z_2$ atoms. If, however, the two $\sigma_i(W)$ do not have the same shape—and there is no reason why they should have—then $A(Z_1,Z_2)$ is indeed dependent on the shape of $n(W)$ unless this shape is independent of composition. Numerical results with a model for condensed matter, yielding a constant energy loss $\Delta W$ of muons impinging on an atom and a maximum angular momentum $I_0$ for muons to be captured, were calculated in Ref. [12]. The effect of $n(W)$ on the initial angular-momentum distribution density $P(I)$ is a little bit more complicated. In the same model the distribution was found to be [12]

$$P\left(\frac{I}{I_0}\right)\frac{dI}{I_0}=\frac{4IdI}{(a+b\Delta W/2)I_0^2}\left[a\ln\frac{I_0}{I}+\frac{b\Delta W}{2}\left(1-\frac{I^2}{I_0^2}\right)\right], \tag{3}$$

where $a$ and $b$ are constants characterizing the deviation of $n(W)$ from a white, i.e., horizontal, spectrum via

$$n(W)=\text{const}\times(a+bW). \tag{4}$$

The effect of $P(I_0)$ within a certain level of the muonic atom on the observable x-ray cascade is calculated numerically with the help of a cascade program; for a review see Ref. [13].

The spectral flux density $n(W)$ at low energies is expected to depend strongly on the nature of the traversed matter, above all whether it is a metal or an insulator [14]: in a metal arbitrarily small energy transfer from the muon to electrons is possible, whereas in an insulator the gap between conduction and valence bands forbids small transfers. Hence the stopping power of a conductor should exceed by far that of an insulator in the case of very slow muons.

Unfortunately there is only one measurement on the muon spectrum at the energies where capture is supposed to mainly take place, and this on a material which is theoretically hard to treat, kapton [15]. The spectral flux density $n(W)$ increases strongly with decreasing energy in the measured range (400 to 1 eV), and, correspondingly the stopping power $\tilde{S}(W)$ decreases [16]; as kapton is an insulator, this behavior is in accordance with the expectations. No measurement exists on $\sigma(W)$. Experimental search for an effect of $S$ on the per-atom capture ratio $A(Z_1,Z_2)$ did not yield a positive result in the case of single-phase Nb-V alloys although $S$ was varied between 0.046 and 18.5 [17]. In the same experiment no variation of the x-ray pattern with $S$ was found.

Cu-Al and Ag-Zn targets with phases depending on the stoichiometric ratio $S$ of the alloys were investigated by Naumann *et al.* [18]. With the exception of the case with the lowest Al concentration, all per-atom capture ratios proved to be concentration independent; the authors do not consider the exception as an example of dependence, since the error here is rather large. The reported Cu x-ray intensity patterns agree for the two targets of the same phase, and show slight, but statistically significant, deviations when the target with another phase is also considered.

In targets containing bound hydrogen and a heavier element $Z$, the higher members of the Lyman series are enhanced compared to a pure $Z$ target, as first observed by Daniel *et al.* [19] (comparison of polyethylene with graphite, and water with metal oxides). In a later experiment on aqueous solutions of alkali halides and the respective solid salts [1] it was conclusively demonstrated that this enhancement is due to transfer and not to the formation of mesomolecular states at the capture process; the mesomolecular state model was advocated for by Gershtein *et al.* [20].

In this work the results of experiments specifically intended to search for alterations of the muonic atomic capture and x-ray cascade processes occasioned by structural variations of the stopping target are reported. We compare muon capture for targets (a) involving different allotropic forms of one element (Se); (b) two crystalline forms of the same ionic salt, one lattice incorporating water molecules ($MgCl_2$, and

$MgCl_2 \cdot 6H_2O$); and (c) binary metallic solutions of varying composition (Nb-Ta alloys). We first want to address the intensity pattern in different allotropic forms, then the same for the salts, and finally the concentration dependence of the per-atom capture ratio in the single-phase Nb-Ta alloys.

## II. TARGETS AND EXPERIMENTS

For the investigation of different allotropic forms, five targets were made. Red and black forms of selenium, the first one freshly prepared, with a purity of greater than 99% were supplied by our radiochemist V. Dornow and by E. Merck and Co., Darmstadt, Germany, respectively. Two targets, red and black selenium, respectively, were contained in aluminum boxes with interior dimensions $70\times50\times2\,mm^3$ equipped with 1.4-mm aluminum windows. The thickness values of these targets were 0.46 and $0.96\,g/cm^2$, respectively. Three further targets of selenium were made using polyethylene frames with dimensions $50\times70\times2.5\,mm^3$ and equipped with 20-$\mu$ Mylar windows; these were red, black, and glassy, the latter also freshly prepared by V. Dornow. The targets had an area density of 0.27, 0.97, and $0.65\,g/cm^2$, respectively; keep in mind that the density of the red Se targets depended largely on the pressure applied at filling. The different frame material allowed us to distinguish clearly between lines that are associated with Se and others which are not. The last three targets had almost no absorption in the windows; on the other hand, the thin mylar windows were to some extent transparent to $H_2O$ vapor while the aluminum boxes were totally sealed. We denote all these targets as Se (I) through Se (V).

Two crystalline forms of magnesium chloride are known; the anhydrous form $MgCl_2$ and the hexahydrate $MgCl_2 \cdot 6H_2O$. The H to Mg and H to Cl ratios of 12 to 1 and 6 to 1, respectively, afforded another opportunity to examine the hydrogen enhancement effect. The magnesium chloride hydrate was supplied by E. Merck and Co. The magnesium chloride (water free) was prepared in our Institute.

Two targets were made, both contained in thin polyethylene sealed target holders with interior dimensions $70\times50\times10\,mm^3$. The values for the thickness of the targets were $0.92\,g/cm^2(MgCl_2 \cdot 6H_2O)$ and $1.08\,g/cm^2(MgCl_2)$. Accordingly, all corrections for self-absorption of the muonic Lyman x rays were negligible.

The tantalum-niobium system forms a continuous series of solid solutions [21]. The alloys were prepared by repeated melting of accurately weighed mixtures of high-purity tantalum and niobium in an arc furnace. The alloys were powdered and placed in boxes constructed with a 2-mm-thick polyethylene frame having interior dimensions $50\times70\,mm^2$, and equipped with 8-$\mu$-thick Mylar windows. Three samples were prepared; cf. Table I.

For all of the alloy systems so far studied, no evidence has been obtained for a change in the relative intensities of the $K$ series with composition. To simplify the evaluation of the more complex $K$ x-ray spectra of the present case, we have evaluated the intensities of only the $K_\alpha$ member $2\rightarrow1$ transition for both the niobium and tantalum, and used these as a basis for evaluating relative per-atom capture ratios. For the case of tantalum, the relative $K_\alpha$ intensity was evaluated from the double escape peak due to the better statistics.

TABLE I. Target composition by mass %, stoichiometric ratio $S$(Ta,Nb), target thickness $d$, measured uncorrected capture ratio $\tilde{R}$(Ta,Nb), and measured uncorrected per-atom capture ratio $\tilde{A}$(Ta,Nb).

| Mass % | $S$(Ta,Nb) | $d$ ($g/cm^2$) | $\tilde{R}$(Ta,Nb) | $\tilde{A}$(Ta,Nb) |
|---|---|---|---|---|
| 17.8 % Ta | 0.111 | 1.02 | $0.132\pm0.004$ | $1.191\pm0.034$ |
| 66.1 % Ta | 1.00 | 1.29 | $1.224\pm0.020$ | $1.224\pm0.020$ |
| 94.6 % Ta | 8.99 | 1.50 | $10.00\pm0.28$ | $1.111\pm0.031$ |

The muonic x-ray spectra were recorded at the muon channel I of the Paul Scherrer Institute, Villigen, Switzerland. A Ge(Li) detector with a volume of $42\,cm^3$ was employed. The stopping telescope and coincidence electronics have been described elsewhere [22]. Since the $K$ muonic x-ray energies for the magnesium chloride and niobium-tantalum systems were high, and since we were interested in relative intensities and relative capture rates, we report for these systems the relative intensities directly recorded by the detector, i.e. uncorrected for intrinsic efficiency; in this way we avoid error correlations. In the case of the selenium targets, where we were also interested in the lower energy $L$ and $M$ series, we report absolute intensities, and have included the needed target absorption corrections.

Figure 1 shows the Paschen series of target Se (I). Note, in particular, that the $O(3\rightarrow1)$ line at 158.41 keV shows up only with a very low intensity; cf. Sec. IV.

## III. RESULTS

Table II summarizes the Lyman series intensities relative to the $2\rightarrow1$ transition from all Se targets. The Balmer and Paschen series have been evaluated only for targets Se (I) and Se (II) as the Se allotropes where discrepancies between previous investigations, (see Refs. [7] and [10]) existed; the results of the present work are listed in Table III.

The constancy of the Lyman and Balmer series from the Se allotropic forms may be rationalized in terms of the local coordination and bonding of the selenium allotropes. In the cases of either the $Se_8$ rings or the long $Se_n$ chains, each selenium atom is bonded to two nearest neighbors through two $\sigma$ bonds. Thus the electronic structure and the local bond lengths should be only slightly affected by the allotropic form. For the higher transitions, which are expected to be more sensitive to outer-electron changes due to, for example, the differing density, this conclusion no longer holds.

The muonic Lyman intensity patterns observed on $MgCl_2$ and $MgCl_2 \cdot 6H_2O$ are shown in Table IV, again with the intensity of the higher members for each element given as a ratio to the intensity of the $K_\alpha$ x ray. The double ratios

$$\mathcal{D}=[I_{n\rightarrow1}/I_{2\rightarrow1}]_{MgCl_2\cdot H_2O}/[I_{n\rightarrow1}/I_{2\rightarrow1}]_{MgCl_2} \qquad (5)$$

for both transitions in Mg and Cl, are also included.

The ratios of the summed up Lyman line intensities $\tilde{R}$(Ta,Nb) not corrected for detector efficiency, measured for the three alloy systems, are listed in Table I together with the atomic ratio $S$(Ta,Nb) calculated from the mass % values

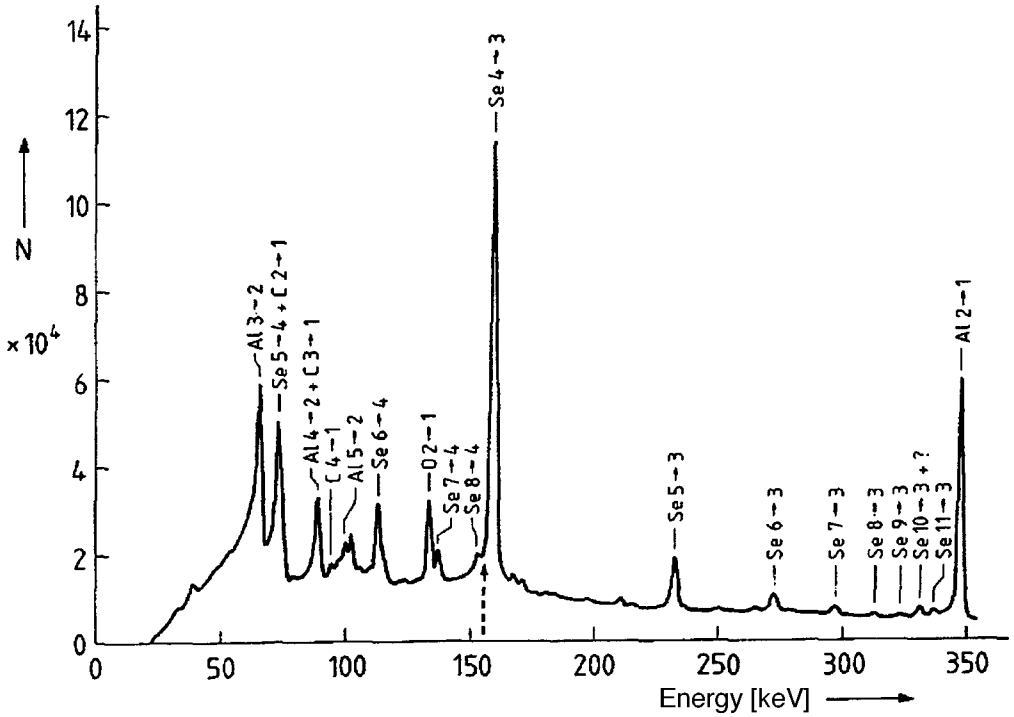


FIG. 1. Paschen series of red Se [target Se (I)]. The dashed arrow indicates the position of an O $(3\rightarrow1)$ contribution.

determined by weighing. The last column shows the, again uncorrected, per-atom capture ratios $\tilde{A}$(Ta,Nb); for this procedure, see Sec. IV.

For the three alloys, an average relative capture ratio $1.18\pm0.06$ may be calculated. On this basis, we conclude that, for the tantalum-niobium alloy system, the per-atom muon capture is invariant at about the 5% level to an 80 fold variation in the atomic ratio. This behavior accords with the other alloy systems previously studied.

## IV. DISCUSSION AND CONCLUSIONS

Considering the question of a variation in the x-ray cascade involving different allotropic forms of one element, Se, (a) of Sec. I, we first look at Table II and state that no difference in the Lyman intensity pattern from all five targets and three modifications outside the experimental errors shows up. This is in disagreement with the Fribourg results [10] (cf. Sec. I). In the Balmer series we again do not recognize an appreciable difference, although there seems to be a preference for crossover transitions in the case of the black Se (Table III). This tendency becomes stronger, and outside any experimental error, for the Paschen series, except for the $9\rightarrow3$ transition (also in Table III). This again disagrees with the Fribourg results [10] but is in line with an old CERN result [7]. The disagreement may be due to the handling of the O$(3\rightarrow1)$ transition by the Fribourg group. This transition shows up with an enormous intensity in their spectrum, indicating a large amount of oxygen in or around the target, probably due to water within the target.

As red Se is an insulator and black Se a conductor, one would expect a spectral density $n(W)$ in red Se, increasing strongly with decreasing $W$ [14], and no such increase in black Se. Consequently the initial population of muonic atom states in red Se should be shifted toward lower angular momentum compared to black Se [12] and thus, one might

TABLE II. Experimental *K*-series intensity ratios from Se allotropes (in percent; errors in parentheses). *Not properly recorded.

| Target | I (red) | II (black) | III (red) | IV (black) | V (glassy) |
|---|---|---|---|---|---|
| $n$ | $I_{n\rightarrow1}/I_{2\rightarrow1}$ | $I_{n\rightarrow1}/I_{2\rightarrow1}$ | $I_{n\rightarrow1}/I_{2\rightarrow1}$ | $I_{n\rightarrow1}/I_{2\rightarrow1}$ | $I_{n\rightarrow1}/I_{2\rightarrow1}$ |
| 2 | 100 | 100 | 100 | 100 | 100 |
| 3 | 6.50 (24) | 6.81 (24) | 7.01 (16) | 6.80(11) | 6.94(13) |
| 4 | 1.32 (10) | 1.30 (7) | -* -* | 1.42 (6) | 1.46 (5) |
| 5 | 0.72 (10) | 0.93 (6) | 0.83 (6) | 0.88 (6) | 0.89 (5) |
| 6 | 0.72 (9) | 0.61 (5) | 0.78 (6) | 0.84 (7) | 0.83 (5) |
| 7 | 0.82 (9) | 0.71 (5) | 0.70 (6) | 0.85 (6) | 0.84 (5) |
| 8 | 0.60 (8) | 0.55 (5) | 0.59 (5) | 0.67 (6) | |
| 9 | 0.71 (8) | 0.71 (5) | 0.71 (5) | 0.73 (7) | |
| 10 | 0.67 (9) | 0.57 (5) | | | |

TABLE III. Experimental *L*- and *M*-series intensity ratios from Se allotropes (in percent).

| Target | I (red) | II (black) | Target | I (red) | II (black) |
|---|---|---|---|---|---|
| $n$ | $I_{n\rightarrow2}/I_{3\rightarrow2}$ | $I_{n\rightarrow2}/I_{3\rightarrow2}$ | n | $I_{n\rightarrow3}/I_{4\rightarrow3}$ | $I_{n\rightarrow3}/I_{4\rightarrow3}$ |
| 3 | 100 | 100 | 4 | 100 | 100 |
| 4 | 13.27 (27) | 14.11 (16) | 5 | 16.42 (19) | 17.75 (23) |
| 5 | 3.34 (14) | 3.34 (8) | 6 | 6.62 (10) | 7.30 (11) |
| 6 | 2.15 (22) | 2.13 (8) | 7 | 2.83 (22) | 3.62 (8) |
| 7 | 1.44 (10) | 1.54 (8) | 8 | 0.99 (8) | 1.16 (6) |
| 8 | 1.06 (9) | 1.17 (7) | 9 | 1.60 (21) | 1.20 (6) |
| 9 | 1.34 (9) | 1.36 (8) | | | |
| 10 | 0.88 (9) | 1.03 (7) | | | |

TABLE IV. Experimental *K*-series intensity ratios from $MgCl_2$ and $MgCl_2 \cdot 6H_2O$ and double ratios $\mathcal{D}$ (not corrected for absorption and detector efficiency; in percent).

| $n$ | Mg $I_{n\to1}/I_{2\to1}$ | | Cl $I_{n\to1}/I_{2\to1}$ | | $\mathcal{D}$ | |
|---|---|---|---|---|---|---|
| | $MgCl_2$ | $MgCl_2 \cdot 6H_2O$ | $MgCl_2$ | $MgCl_2 \cdot 6H_2O$ | Mg | Cl |
| 2 | 100 | 100 | 100 | 100 | 1.00 | 1.00 |
| 3 | 7.23 (17) | 8.89 (34) | 6.50(10) | 7.74 (18) | 1.23 (6) | 1.19 (3) |
| 4 | 4.44 (15) | 6.46 (32) | 2.53 (6) | 3.12 (12) | 1.46 (9) | 1.23 (5) |
| 5 | 3.05 (17) | 5.15 (30) | 2.29 (6) | 3.43 (16) | 1.69 (13) | 1.49 (7) |
| 6 | 1.85 (14) | 3.00 (26) | 1.83 (5) | 2.55 (11) | 1.62 (19) | 1.39 (7) |
| 7 | 1.26 (12) | 1.89 (27) | 1.05 (4) | 1.79 (10) | 1.49 (26) | 1.69 (11) |
| 8 | | | 0.50 (3) | 0.78 (18) | | 1.56 (20) |

think, yield higher crossover intensities, in contradiction to the observation (Table II). However, the physical state of the target also affects the muonic x-ray cascade. Decisive is the refilling rate of vacancies produced by Auger transitions [21]. Although even within an insulator there are enough electrons present to fill vacancies produced in the valence band or in a localized atomic state—in this sense the insulator does not really insulate, as it allows charge transport into the vacancy—the refilling is expected to be much slower than in a conductor as energy and angular momentum are not easily taken away. This means an electron deficiency around the muonic atom, and hence an increase of the intensity of the radiative transitions compared to the Auger transitions in the upper part of the cascade. These radiative transitions then mostly lead to circular orbits and, hence, a lower population of the low-lying noncircular states whose deexcitation crossover transitions can be observed.

The theories of Coulomb capture and subsequent x-ray cascade of muons in condensed matter are not developed enough to allow the detailed calculation of the x-ray pattern or to relate this pattern to the electronic structure. Hence no comparison with theory is possible.

The next point, (b) of Sec. I, mainly concerns the role of hydrogen. One recognizes a large enhancement of the crossover lines [double ratio ($\mathcal{D}$) in Table IV]. These enhancements displayed in Table IV are comparable to the effects we have previously observed for the four-molar aqueous solutions [1]. The present observation of enhancements for both the magnesium cation (predominantly adjacent to oxygen atoms of the coordinated water molecules) and the chlorine atoms (predominantly adjacent to hydrogen atoms) directly support our previous conclusion that transport of neutral $\mu$-mesic hydrogen systems account for the *K* x-ray intensity variations. In our solution studies, we had inferred a sequence involving (a) formation of excited $\mu$-mesic hydrogen atoms, (b) diffusion of these atoms over lengths exceeding the 9.6-nm H—O bond length of the water molecule, and (c) Coulomb stripping of the muonic hydrogen atom in the field of a high-$Z$ nucleus. In $MgCl_2 \cdot 6H_2O$ each Mg atom is octahedrally surrounded by six water molecules at a distance of 20.1–20.7 nm, and each Cl atom has eight water neighbors; six of these have separations between 32.1 and 32.8 nm, while the other two are 35.3 nm [23]. The enhancements we report here give additional evidence for the muonic hydrogen atom transport mechanism [1].

As we were mainly interested in the search for variations of the per-atom capture $A(Z_1,Z_2)$ with the concentrations, (c) of Sec. I, we tried to keep the errors as small as possible. In particular, common efficiency errors which would enter into all measured three capture ratios $A$(Ta, Nb) as correlated errors, and thus maybe mask a concentration dependence, were avoided by not correcting the Lyman lines series intensities for the detector efficiency. Hence the uncorrected ratio $\tilde{A}$(Ta,Nb) is given in Table I. We are aware of the disadvantage: (1) no true capture ratio, to be compared with theory, is available; and (2) in the case of a dependence of the Lyman intensity pattern on the concentration there is the possiblity of inducing a certain error in $\tilde{A}$(Ta, Nb). We consider this possible error as negligible: $\tilde{A}$(Ta, Nb) is predominantly determined by the $K_\alpha$ line, and above all, a variation of the Lyman pattern has not been observed in our experiment.

An inspection of Table I shows a variation of $\tilde{A}$(Ta,Nb) that is, although small, outside the errors. We do state, however, that the deviations from the mean, $\langle\tilde{A}(\mathrm{Ta,Nb})\rangle = 1.18 \pm 0.06$, do not exceed 5%. It is interesting to note that for a totally different class of condensed matter, glasses of various compositions, an approximate constancy of the per-atom capture ratios had also been observed [24].

In summarizing our findings we state that the change of modification and composition has a small but detectable effect on the x-ray intensities and capture probabilities in solid targets. Moreover, the transfer from hydrogen in the aqueous solution changes the intensities of crossover transitions drastically compared to the solid compound.

[1] H. Daniel, F. J. Hartmann, R. A. Naumann, and J. J. Reidy, Phys. Rev. Lett. **56**, 448 (1986).

[2] T. von Egidy, W. Denk, R. Bergmann, H. Daniel, F. J. Hartmann, J. J. Reidy, and W. Wilhelm, Phys. Rev. A **23**, 427 (1981).

[3] H. Schneuwly, in *Exotic Atoms in Condensed Matter*, edited

by G. Benedek and H. Schneuwly (Springer, Berlin, 1992).
[4] S. Stanislaus, F. Entezami, A. Bagheri, D. F. Measday, and D. Garner, Nucl. Phys. A **475**, 630 (1987).
[5] R. A. Naumann, H. Daniel, P. Ehrhart, F. J. Hartmann, and T. von Egidy, Phys. Rev. A **31**, 727 (1985).
[6] H. Daniel and R. A. Naumann, Z. Phys. A **291**, 33 (1979).
[7] L. Tauscher, G. Backenstoss, S. Charalambus, H. Daniel, H. Koch, G. Poelz, and H. Schmitt, Phys. Lett. **27A**, 581 (1968).
[8] J. D. Knight, C. J. Orth, M. E. Schillaci, R. A. Naumann, H. Daniel, K. Springer, and H. B. Knowles, Phys. Rev. A **13**, 43 (1976).
[9] H. Schneuwly, M. Boschung, K. Kaeser, G. Piller, A. Ruetschi, L. A. Schaller, and L. Schellenberg, Phys. Rev. A **27**, 950 (1983).
[10] K. Kaeser, T. Dubler, B. Robert-Tissot, L. A. Schaller, L. Schellenberg, and H. Schneuwly, Helv. Phys. Acta **52**, 238 (1979).
[11] H. Daniel, Ann. Phys. (N.Y.) **129**, 303 (1980).
[12] H. Daniel, Z. Phys. A **302**, 195 (1981).
[13] F. J. Hartmann, in *Electromagnetic Cascade and Chemistry of Exotic Atoms*, edited by L. M. Simons, D. Horváth, and G. Torelli (Plenum, New York, 1990), p. 127.
[14] W. Schott, H. Daniel, F. J. Hartmann, and W. Neumann, Z. Phys. A **346**, 81 (1993).
[15] H. Daniel, F. J. Hartmann, W. Neumann, and W. Schott, Phys. Lett. A **191**, 155 (1994).
[16] H. Daniel, Nucl. Instrum. Methods **147**, 297 (1977).
[17] R. Bergmann, H. Daniel, T. von Egidy, F. J. Hartmann, J. J. Reidy, and W. Wilhelm, Phys. Rev. A **20**, 633 (1979).
[18] R. A. Naumann, G. Schmidt, J. D. Knight, L. F. Mausner, C. J. Orth, and M. E. Schillaci, Phys. Rev. A **21**, 639 (1980).
[19] H. Daniel, H. Koch, G. Poelz, H. Schmitt, L. Tauscher, G. Backenstoss, and S. Charalambus, Phys. Lett. **26B**, 281 (1968).
[20] S. S. Gershtein, V. I. Petrukhin, L. I. Ponomarev, and Yu. D. Prokoshkin, Usp. Fiz. Nauk **97**, 3 (1969) [Sov. Phys. Usp. **12**, 1 (1969)].
[21] M. Hansen and K. Anderko, *Constitution of Binary Alloys* (McGraw-Hill, New York, 1958), p. 1018.
[22] F. J. Hartmann, R. Bergmann, H. Daniel, H. J. Pfeiffer, T. von Egidy, and W. Wilhelm, Z. Phys. A **305**, 189 (1982).
[23] R. W. G. Wyckoff, *Crystal Structures*, 2nd ed. (Interscience, New York, 1965), p. 785.
[24] H. Daniel, F. J. Hartmann, and E. Köhler, Fresenius Z. Anal. Chem. **321**, 65 (1985).